

RESEARCH LETTER

10.1002/2015GL063809

Key Points:

- Geometric constraints show seafloor channels to be inherently unstable
- Stability under inherent forcing decreases with progressive deposition
- Stability under imposed forcing also decreases with progressive deposition

Supporting Information:

- Text S1

Correspondence to:

R. M. Dorrell,
r.m.dorrell@leeds.ac.uk

Citation:

Dorrell, R. M., A. D. Burns, and W. D. McCaffrey (2015), The inherent instability of leveed seafloor channels, *Geophys. Res. Lett.*, 42, 4023–4031, doi:10.1002/2015GL063809.

Received 10 MAR 2015

Accepted 27 APR 2015

Accepted article online 2 MAY 2015

Published online 22 MAY 2015

The inherent instability of leveed seafloor channels

Robert M. Dorrell¹, Alan D. Burns², and William D. McCaffrey¹

¹School of Earth Sciences, University of Leeds, Leeds, UK, ²School of Chemical and Process Engineering, University of Leeds, Leeds, UK

Abstract New analytical models demonstrate that under aggradational flow conditions, seafloor channel-levee systems are inherently unstable; both channel area and stability necessarily decrease at long timescales. In time such systems must avulse purely through internal (autogenic) forcing. Although autogenic instabilities likely arise over long enough time for additional allogenic forcing to be expected, channel-levee sensitivity to variations in flow character depends on the prior degree of system evolution. Recalibrated modern Amazon Fan avulsion timings are consistent with this model, challenging accepted interpretations of avulsion triggering.

1. Introduction

Gravity currents are flows driven by a density difference from the surrounding fluid; in submarine environments, this difference may be generated through suspended sediment load, temperature, or salinity [Simpson, 1999]. Particle-laden gravity currents, such as turbidity currents and debris flows, are the primary means of redistributing sediment from shallow to deep marine environments.

Turbidity currents are often confined in channels, bounded by self-regulated levees [Buffington, 1952]. Such channel-levee systems are most commonly found in association with mud-rich sediment sources [Saller and Dharmasamadhi, 2012]. Similarly to fluvial systems, seafloor channels may avulse, allowing gravity currents to travel along new pathways; the original channel downstream of the avulsion point may immediately or progressively become abandoned. Networks of such channels form submarine fans, some of the largest sedimentary deposits in the world [Covault, 2011].

Submarine fans develop through interplay of internal (autogenic) and external (allogenic) controlling factors. Allogenic variations in the flows (random and/or cyclical) have a significant effect on system style [Kolla, 2007]; however, the role of autogenic constraints on channel evolution is not well constrained. Critically, it is unapparent whether allogenic forcing, such as sea level change, must be invoked to explain channel avulsion.

2. Controls on Seafloor Channel Stability and Avulsion

Key to understanding the characteristic architecture of submarine fans is the process of seafloor channel avulsion, which limits channel growth and increases submarine fan complexity. Allogenic forces driving channel avulsion include seafloor uplift [Clark and Cartwright, 2011; Chiang *et al.*, 2012], flow boundary condition (sea level) change [Lopez, 2001; Maslin *et al.*, 2006; Kolla, 2007], or channel occlusion by debrites [Kolla, 2007; Wynn *et al.*, 2007]. Autogenic channel avulsion only arises if the flow and bounding topography evolve toward a state of disequilibrium.

To understand the causes of seafloor channel instability and avulsion, it is necessary to assess the interplay of flow dynamics and confinement within leveed channels. Turbidity currents are generally stratified in terms of velocity, suspended sediment concentration, and grain size [Peakall *et al.*, 2000], with a proportion of the flow covering the leveed channel [Kane *et al.*, 2010a, 2010b]. Mohrig and Buttles [2007] note that flows effectively become unconfined when above a critical flow to channel depth ratio and associate this limit to superelevation of the velocity maximum above the height of the confining levees, *i.e.*, before full channel occlusion. Thus, as the ratio of confinement to flow area decreases, the likelihood of channel avulsion increases. If the depositional behavior of a flow varies across a leveed channel, it is apparent that the system may be inherently unstable (*e.g.*, depositional in-channel and erosional on levee) or inherently stable (*e.g.*, erosional in-channel and depositional on levee). However, the stability state is unapparent while a flow is uniformly depositional

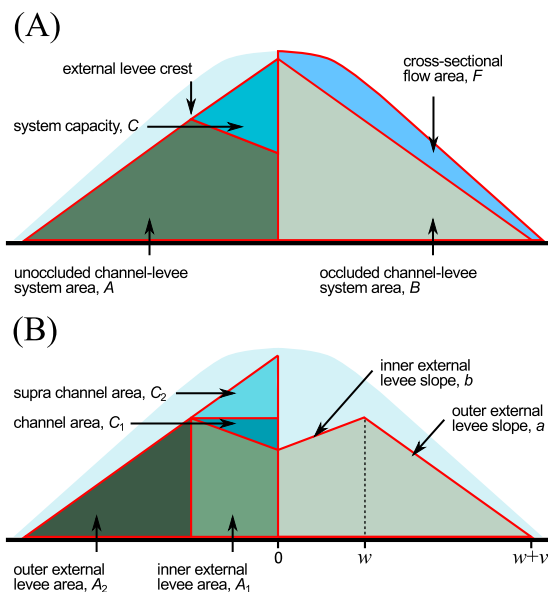


Figure 1. (a) Cross-sectional transect of a conceptual leveed seafloor channel system, described in terms of its occluded, A , and unoccluded, B , state. (b) Key geometric parameters detailing width and slope of the bounding inner and outer external levee [Kane and Hodgson, 2011]. Model assumptions are summarized in the supporting information.

or erosional. The analysis presented here focuses on the case where flows are depositional across both channel and levees, i.e., downdip of any slope erosion-deposition equilibrium point [Kneller, 2003]; the frequently observed coelevation of channel and associated levees seen in many seismic studies suggests that this is commonly the case [e.g., Damuth et al., 1988; Covault, 2011].

3. Inherent Channel Stability

Here a conceptual two-dimensional cross-sectional model of a leveed seafloor channel is defined by a centrally located channel thalweg and a master bounding external levee [Kane and Hodgson, 2011] (Figure 1a). The initially unoccluded channel acts as a conduit to system-traversing flow, whose cross-sectional area, from the system center outward, is defined $F(t)$; the area of the unoccluded leveed channel is defined $A(t)$. In the limit of complete channel occlusion the system comprises only the bounding levee, with a comparative center to cross-sectional area $B(t)$. The difference between occluded and unoccluded systems, $C(t)$, is

$$B(t) - A(t) = C(t). \tag{1}$$

The unoccluded leveed channel area may be split into two regions, $A(t) = A_1(t) + A_2(t)$; where after Kane and Hodgson [2011], the region between the centrally located thalweg and the external levee crest is denoted by the inner external levee, $A_1(t)$, while the region between the external levee crest and the lateral extent of the bounding levee is denoted by the outer external levee, $A_2(t)$. In similar fashion $C(t) = C_1(t) + C_2(t)$, where $C_1(t)$ is the bankfull channel area, below the master bounding levee, and $C_2(t)$ the suprachannel area (Figure 1b).

Here four key geometric parameters are assumed to fully describe these regions: the outer, $v(t)$, and inner, $w(t)$, external levee width and the mean outer, $a(t)$, and inner, $b(t)$, external levee slope, see Figure 1b. After the model of Spinewine et al. [2011], levee slopes are assumed planar. For brevity, time dependence notation is henceforth omitted. In terms of the cross-sectional position from the system center, x , the bed depth, $\eta(x, t)$, has the assumed form

$$\eta(x, t) = \begin{cases} a(t)v(t) - b(t)(w(t) - x) & 0 \leq x < w(t) \\ a(t)(w(t) + v(t) - x) & w(t) \leq x < w(t) + v(t) \\ 0 & \text{otherwise} \end{cases}, \tag{2}$$

defining the areas $A_1 = awv - bw^2/2$, $A_2 = av^2/2$, $C_1 = bw^2/2$, $C_2 = aw^2/2$. Moreover, $C \equiv (1 + a/b)C_1$ and is therefore a measure of the capacity of the system to act as a flow conduit; C is henceforth referred to as system capacity.

Although seafloor channels are constructed by many transient turbidity currents events, the morphodynamic effects of short-lived flow heads and tails may be neglected compared to those of the longer-lived flow bodies [e.g., Pirmez and Imran, 2003]. Thus, the cumulative effect of individual flow events is modeled as arising from quasi-continuous flow [Spinewine et al., 2011] and at any point in space, x , and time, t ; the change in the bed depth is

$$\frac{d}{dt}\eta(x, t) = N_0(x, t), \tag{3}$$

where $N_0(x, t)$ is the net rate of deposition, divided by the change in concentration between the bed and the suspension [cf., *Dorrell et al.*, 2013]. Respectively, the instantaneous and time integrated rate of change in the leveed channel area, A , are

$$N_1(t) = \int_0^\infty N_0(x, t) dx \quad \text{and} \quad N_2(t) = \int_0^t N_1(t') dt'. \quad (4)$$

In uniformly aggradational flows N_0 (3), N_1 and N_2 (4) are greater than zero, while in erosional flows they are less than zero. Given the focus here on depositional, channel building systems, the analysis presented is limited to purely aggradational flows.

The change in the area of the inner and outer external levees, A_1 and A_2 , respectively, is given from the integrated rate of deposition (3) between zero and w and w and infinity, respectively.

$$\int_0^{w(t)} \frac{d}{dt} \eta(x, t) dx = \frac{dA_1}{dt} - av \frac{dw}{dt} = (1 - E)N_1(t), \quad (5)$$

$$\int_{w(t)}^\infty \frac{d}{dt} \eta(x, t) dx = \frac{dA_2}{dt} + av \frac{dw}{dt} = EN_1(t), \quad \text{and} \quad (6)$$

$$E = \frac{\int_{w(t)}^\infty N_0(x, t) dx}{N_1(t)}. \quad (7)$$

In (5) and (6) E denotes the dimensionless fraction of material deposited outside the channel; $1 - E$ is the fraction of material deposited in channel. The cases $E = 0$ and $E = 1$, respectively, correspond to flow with no deposition on the outer external levee (fully confined by the channel) and flow with no deposition on the inner external levee (bypassing). In (5) and (6) $av d/dt w$ describes the effect of levee crest migration on change of levee area (see supporting information for full derivation of (5) and (6)). Although the solutions depicted herein are symmetric about the thalweg, (5) and (6) describe half of the channel-levee system and thus can be generalized to nonsymmetric forms.

The progression of the leveed channel system toward an occluded or increasingly unoccluded state is given by the change of system capacity in time (1). From (5) and (6),

$$\frac{d}{dt} C = S + D, \quad S = w \frac{w + v}{2} \frac{d}{dt} a, \quad D = wN_1 \left(\frac{E}{v} - \frac{1 - E}{w} \right), \quad (8)$$

(for derivation, see supporting information) where S denotes the change in C via outer external levee steepening and D the difference between the rate of sedimentation per unit width on the outer and inner external levees.

During aggradational flow, levee steepening is expected. However, they cannot steepen indefinitely and the slopes thus tend to some equilibrium value, i.e., $S \rightarrow 0$; such limiting behavior is observed both experimentally and in seismic [*Straub et al.*, 2008; *Straub and Mohrig*, 2008]. The limit $S \rightarrow 0$ may be controlled by the intrinsic shear strength of the levee sediment and by depositional or erosional flow processes [*Audet*, 1998; *Kane et al.*, 2010a; *Sawyer et al.*, 2014]. When S is assumed to be negligible (or the slope shallows, S negative) and while the net deposition per unit width is greatest on the inner external levee, i.e., D is negative, system capacity, C , must decrease and the system must become increasingly occluded. Conversely system capacity can only increase while net deposition per unit width is greatest on the outer external levee, i.e., D is positive, and/or the outer external levee(s) steepen.

While the outer external levee is much wider than the inner external levee defining the channel [see, e.g., *Damuth et al.*, 1988], net deposition per unit width, D , may be assumed to be negative as wE/v may be assumed to be smaller than $1 - E$. Following the argument above, this implies that the capacity of channel-levee systems to act as a flow conduit decreases during aggradational flow conditions.

The foregoing analysis suggests that aggradational channels are inherently unstable, as system occlusion forces disequilibrium between the flow conditions and the confining topography, e.g., the channel infills as it is built up quicker than the bounding levees. Such disequilibrium flow is increasingly super elevated above

the channel, increasing the likelihood of levee breaching conditions and therefore avulsion. However, in a bypassing flow, $E \rightarrow 1$, it is not immediately apparent whether wE/v is less than $1 - E$ and thus if the channel is inherently unstable or not (8). To examine system stability in this limit, it is necessary to derive late time solutions to (8).

4. Model Solutions of Seafloor Channel Evolution

As there are four unknowns, a , b , v , and w , but only two equations describing channel evolution, (5) and (6), simplifying assumptions must be made to close the system. Here it is assumed that the initial model boundary condition is taken at some point after the development of a channel-levee system, such that the levee slopes have evolved to some constant value, as discussed above. Accordingly, the inherent stability of a channel system can be directly assessed by integrating (5) and (6). From (4) $A(t) = A(0) + N_2(t)$, while (1) may be rewritten in terms of nondimensional variables as follows

$$\tilde{B}(t) = \frac{B(t)}{A(t)}, \quad \tilde{C}(t) = \frac{C(t)}{A(t)} \quad \text{such} \quad \tilde{B}(t) - \tilde{C}(t) = 1. \quad (9)$$

Given (9) the channel stability equation (8) may be expressed in terms of \tilde{C} and reduced to a nonautonomous ordinary differential equation of the form,

$$\frac{A(t)}{N_1(t)} \frac{d}{dt} \tilde{C}(t) = \frac{E - 1 - \tilde{C}(t) + \sqrt{\frac{\gamma}{\gamma+1}} \sqrt{\tilde{C}(t)} \sqrt{\tilde{C}(t) + 1}}{1 - \sqrt{\frac{\gamma}{\gamma+1}} \frac{\sqrt{\tilde{C}(t)}}{\sqrt{\tilde{C}(t)+1}}}. \quad (10)$$

Here $\gamma = a/b$ denotes the ratio of the outer to inner external levee slope. For fixed E , (10) may be simplified into an autonomous ordinary differential equation. However, while channel geometry (or flow magnitude) varies, the fractionation of deposited material, E , must also vary, as the degree by which the flow is constrained by the channel changes. Here it is assumed that the flow in-channel is trapped by the bounding channel walls, and thus, material in suspension below the external levee crests can only be deposited on the inner external levee. It is further assumed that the remaining flow is readily stripped to the outer external levee, and thus, material suspended in flow elevated above the levee crests is deposited on the outer external levee. Thus, the ratio of material deposited on the inner versus the outer external levee is assumed to be proportional to the ratio of half-channel area, C_1 , to the remaining area of the flow,

$$\frac{1 - E(t)}{E(t)} = \max \left(\alpha \frac{C_1(t)}{F(t) - C_1(t)}, 0 \right). \quad (11)$$

Here α is a dimensionless constant of proportionality describing the efficiency of flow and sediment fractionation between the inner and outer external levee; α prescribes an initial fractionation value of material deposited on the outer external levee, $E(0)$, given channel area $C_1(0)$ and flow area $F(0)$. In (11) the ratio of deposition on the inner and outer external levee is limited such that if the cross-sectional area of the flow is less than that of the channel, $F < C_1$, there is no deposition on the outer external levee and $E = 0$.

Using (10) and (11), the evolution of the system may be expressed by a phase portrait $[d/dt F/A, d/dt \tilde{C}]$ which describes an attracting locus, \tilde{C}_a , whose position is determined by the equation $d/dt \tilde{C} = 0$ (Figure 2a). The curve $\tilde{C} = \tilde{C}_a$, toward which solutions of the system tend, is seen to monotonically decrease at long time (Figure 2b). At long time, when the total amount of material deposited has built the channel-levee so that it is much larger than the flow, $A \gg F$, then it can be shown that \tilde{C}_a scales inversely with A^2

$$\tilde{C}_a(t) \sim \frac{1}{\alpha^2} \gamma(\gamma + 1) \frac{F^2}{A^2} + \dots \quad (12)$$

(for derivation of (12), see supporting information.) While $\tilde{C} \rightarrow \tilde{C}_a$ (Figure 2) and $\tilde{C} = C/A$ (9), equation (12) implies that both system capacity and bankfull channel area scale inversely with the summed system area, A . Thus, the system must tend toward an occluded state, e.g., $C/F \rightarrow 0$ as $A \gg F$ with progressive deposition (12). It is therefore concluded that the capacity of the system to act as a flow conduit decreases and aggradational leveed channel systems are inherently unstable.

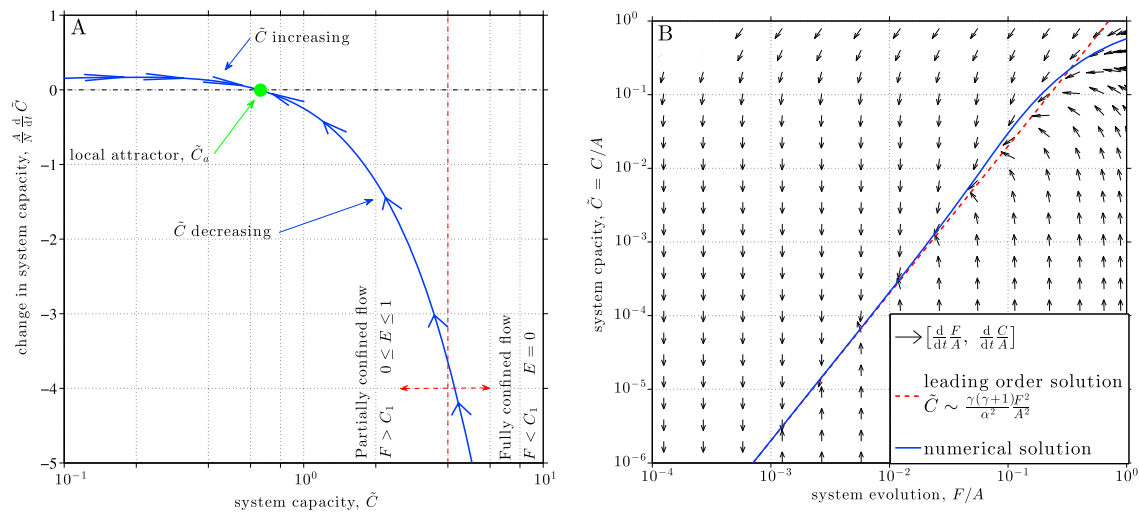


Figure 2. (a) Normalized rate of change of dimensionless system capacity \tilde{C} (10). (b) Temporal evolution of the global attractor, \tilde{C}_a , as described by the vector field plot $d/dt[F/A, C/A]$ (arrows) of the nonautonomous system, (10), numerical (solid blue curve) and leading order analytical solutions in the asymptotic regime $F \ll A$ (12) (red dashed curve). In Figures 2a and 2b $a = b = 0.025$, $v(0) = w(0) = 500$ m, $F = 2C(0)$, $N_1 = 1$ m²s⁻¹, and $\alpha = 1$.

The decrease in C arises because complete flow bypass in the channel (where $E = 1$ and the channel is inherently stable as it does not infill) can never be achieved during the aggradational flow considered. If E decreases toward zero, the channel rapidly fills. If E tends to unity predominately, more material is deposited on the outer external levee, increasing the area, and thus width, faster than that of the inner external levee, (5) and (6). As E is strictly less than unity and as the inner to outer external levee width ratio progressively decreases, deposition per unit length on the outer external levee must eventually become smaller than deposition per unit length on the inner external levee. Thus, channel area, C , and system stability, must eventually decrease, (8).

While the channel system is only occluded completely as its area tends to infinity, (12), the system becomes inherently unstable as the channel decreases in area [Mohrig and Buttles, 2007]. The half life over which the area of C decreases by a factor of 2, Δt , is given by the implicit equation $C(t) = 2C(t + \Delta t)$, which given (12) may be simplified to,

$$\int_t^{t+\Delta t} N_1(t') dt' \sim A(t). \tag{13}$$

From (13) it may be concluded that Δt increases with progressive deposition, e.g., an increase in A , but decreases with increased net deposition rate, N_1 .

5. Discussion

Key to describing the evolution of the channel is the fractionation between material deposited on the inner and outer external levee (11). Although the fractionation of deposited material behaves as a function of the change in channel area, (11), different systems may have different characteristic sediment fractionation, $E(0)$. For example, variation in $E(0)$ will be partially controlled by topographic constraints, such as channel meandering [Straub et al., 2011] and flow stratification (mass lost overbank decreases with increasing stratification [Dorrell et al., 2014]; i.e., E decreases as stratification increases). Sediment fractionation-dependent, late stage evolution of an aggradational channel-levee system is depicted in Figure 3 (geometry is assumed constant). Unstable, upward narrowing channels [see, e.g., Pirmez et al., 2000; Deptuck et al., 2003; Silva, 2011] (Figure 3a) are formed when deposition per unit width is greatest on the inner external levee. Stable, upward widening channels [see, e.g., Silva, 2011] are initially formed as sediment fractionation increases to the point where the outer external levee is initially built up quicker than the inner external levee (Figure 3b). However, such behavior is transient and eventually the system must become occluded.

Figures 3c and 3d depicts channel-levee evolution during flows of waxing-waning size, representative of changing boundary conditions to the channel system [Kolla, 2007]. For simplicity the flow is assumed to be purely aggradational, and the net deposition rate, N_1 , is assumed proportional to the area of the flow

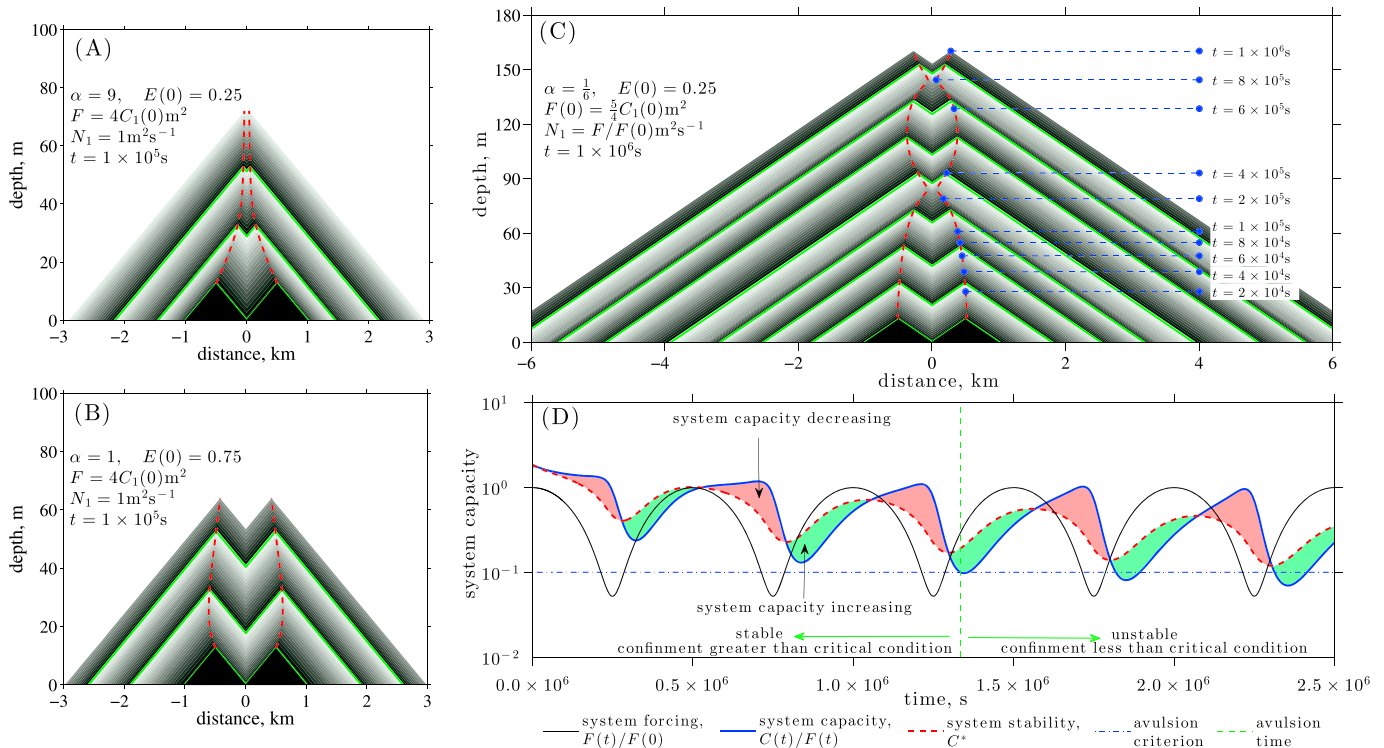


Figure 3. The initial evolution of seafloor channels for varying initial sediment fractionation, α , for (a and b) fixed flow magnitude and (c) varying flow magnitude, given fixed initial sediment fractionation. In Figures 3a–3c red curves denote levee crest location, striped bands denote evolution with progressive deposition, green curves denote depositional contours every 20 m, and blue dashed curves denote evolution time; the initial channel form is shaded black. (d) The evolution of relative system capacity (thick blue curve) and associated system stability curve (14) (thick dashed red curve) for the varying flow magnitude (thin black curve) scenario depicted in Figure 3c; the shaded regions between the system capacity and stability criterion curves highlight the rate of change of system capacity (red decreasing, green increasing). Channel avulsion is assumed only to be possible when the relative capacity, C/F , drops below some (assumed) critical threshold $\lambda = 0.1$ (thin dash-dotted blue curve), setting a minimum avulsion time (thin green dashed curve) for the system.

(i.e., larger magnitude flows deposit proportionally more than smaller flows). As explained above, the global system trend is for a decrease in the system capacity, i.e., increasing system occlusion. However, this may be temporarily reversed by changing flow conditions. Decrease in system occlusion occurs when increased fractionation during waxing flow (11) temporarily offsets the decreasing inner to outer levee width ratio. Equations (8) and (11) set a system stability criterion for decreasing occlusion, C^* , on relative system capacity, the ratio of current system capacity to flow area, C/F , where

$$\frac{dC}{dt} > 0 \quad \text{if} \quad \frac{C}{F} < \tilde{C}^*, \quad C^* = \frac{\gamma + 1}{1 - \alpha + \sqrt{\frac{\gamma + 1}{\gamma} \frac{1 + C}{C}}}, \quad (14)$$

and vice versa. Figure 3d plots the changing stability criterion of the waxing-waning flow depicted in Figure 3c. The model results show that changing relative system occlusion lags behind changing system forcing, e.g., flow magnitude, with decrease in occlusion occurring predominately on the increasing leg. The importance of the periodically varying, but net decreasing, degree of system occlusion is seen with reference to an assumed avulsion threshold, $C \leq \lambda F$, when flow becomes sufficiently poorly constrained that it may avulse [Mohrig and Buttles, 2007]. In Figure 3d it is apparent that the minimum avulsion threshold, $C/F = \lambda$, may not be met until late time, after several cycles of system forcing. This simple model highlights that channel stability may be limited by the current state of evolution of the system, suggesting that significant system forcing may not immediately result in channel avulsion.

Quaternary seafloor channel avulsions of the Amazon Fan (Figure 4) provides a test of this model. Located off the Brazilian continental margin, the Amazon Fan is the third largest mud-rich fan in the world [e.g., Flood et al., 1995]. The distribution of the nine most recent channel-levee complexes and their avulsions was described by Pirmez and Flood [1995] and dated by Maslin et al. [2006]. In Figure 4 recalculated avulsion dates are plotted against associated sea level curves [Wright et al., 2009; Stanford et al., 2011; Miller et al., 2011; Grant et al., 2012, 2014].

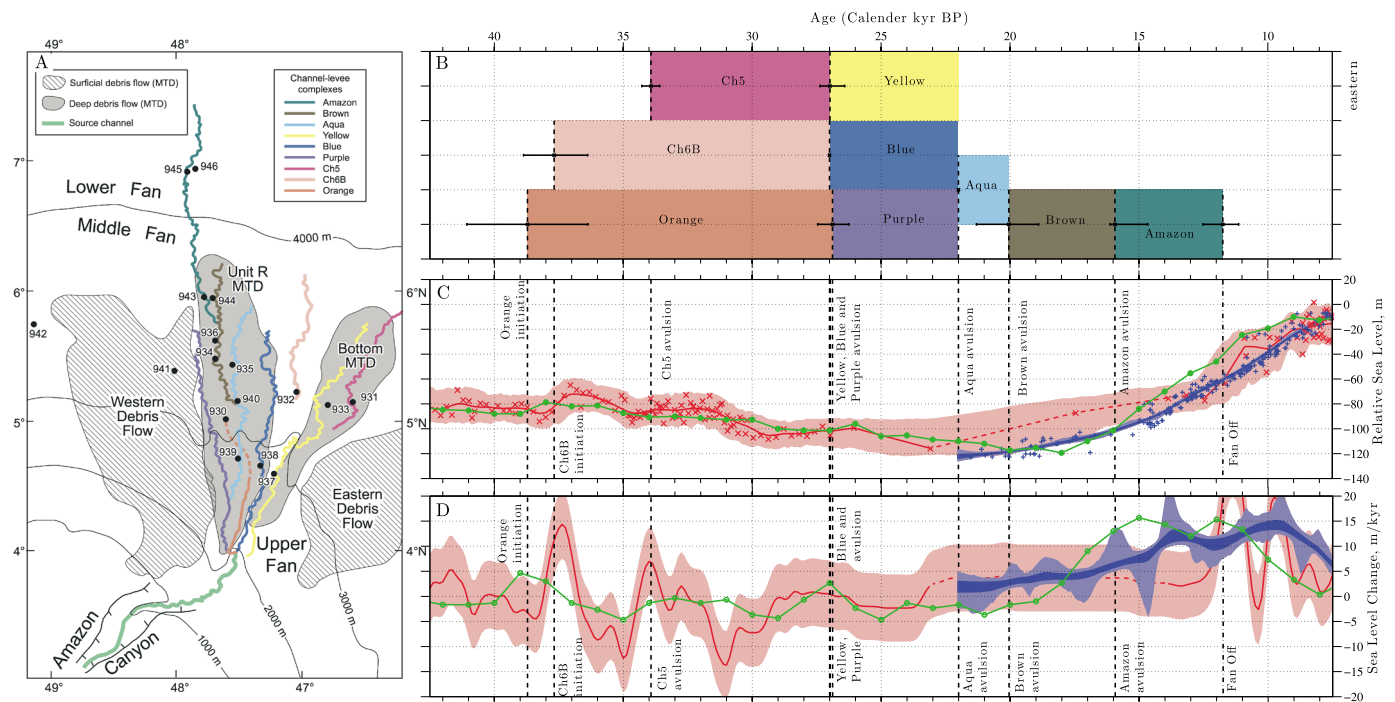


Figure 4. (a) Map of the Amazon seafloor channel network and mass transport deposits, after *Maslin et al.* [2006]. (b) Radiocarbon-based age of channel avulsions in Amazon seafloor fan [*Maslin et al.*, 2006], calculated using OxCal 4.2 [*Ramsey*, 2009; *Reimer et al.*, 2013] and for blue and aqua channel avulsions, palaeomagnetic remanent features and oxygen isotopes [*Maslin*, 2009]. Where multiple radiocarbon data are available, the mean avulsion age is calculated using the Bayesian-based combine function in OxCal; error bars plot the maximum avulsion date range. (c) Probabilistic relative sea level and (d) rate of sea level change during the Quaternary, replotted from the Caribbean study of *Stanford et al.* [2011] (colored blue) and the Red Sea study of *Grant et al.* [2012, 2014] (colored red); the confidence maximum is denoted by solid curves, with the 95% interval shaded. The green curve denotes the interpolated sea level based on the Huon peninsula-Papa New Guinea-Barbados study of *Wright et al.* [2009] and *Miller et al.* [2011].

Maslin et al. [2006] argue that stable bifurcation or trifurcation nodes existed from circa 39–22 kyr B.P., such that the Orange and Channel 6b channels were synchronously active, together with Channel 5, which initiated later (circa 34 kyr B.P.). Dating errors prevent a clear analysis of whether sea level triggering is implicated in the initiation of the older two channels; the younger one appears to have initiated during a period of static sea level. None of these channels avulsed during periods of significant sea level fall (37–34.5 and 32–29.5 kyr B.P.). All three channels appear to have avulsed, either synchronously or in close succession, at around 27 kyr B.P., following a circa 2.5 kyr interval of essentially static sea level. Similarly, the three successor (purple, blue, and yellow) channels were stable during their early history under a regime of falling sea level (26–22 kyr B.P.) and then avulsed synchronously at circa 22 kyr B.P. during a period of static sea level or early rise, initiating a single-channel mode for the fan. The resultant blue channel avulsed under a regime of steadily and slowly rising sea level at circa 20 kyr B.P. as did the successor brown channel (circa 16 kyr B.P.); the resultant Amazon channel remained active until the fan shut down at circa 12 kyr B.P., when the sea flooded back across the shelf, and direct delivery of sediment to the deep sea ceased [*Maslin et al.*, 2006; *Jegou et al.*, 2008].

Contrary to the interpretation of *Maslin et al.* [2006] and *Maslin* [2009], the nine most recent Amazon Fan channel-levee complexes do not show a close association between avulsion and sea level change. The majority of avulsions occur during periods of static sea level or of gentle progressive sea level rise. This observation is consistent with the foregoing analysis, such that channels did not avulse with sea level change in their early history as they had not aggraded close to their autogenic avulsion limit. When avulsion did occur, the channels may have been sufficiently close to that limit to become unstable without any change in flow conditions.

The time taken for a channel to evolve close to an autogenic limit depends on the sedimentation rate (13). It can be noted that the aqua channel was active for around only 2 kyrs, compared to 5 kyrs for the precursor purple, blue, and yellow channels; the shorter duration of the younger channel may reflect development of a single-channel mode. However, the youngest two channels were active for longer, c. 4 kyrs for the Brown channel before avulsion and c. 4 kyrs for the Amazon channel without avulsion when an activity ceased.

The longer duration of progressively younger channels might reflect net reductions in sediment flux to the fan under a rising sea level regime. Further work characterizing the entire fan, i.e., encompassing its distal and terminal lobes reaches [e.g., *Jegou et al.*, 2008] is required to test this conjecture.

6. Conclusions

New models describing the evolution of generic cross-sectional transects of seafloor channel-levee systems demonstrate that seafloor channels are inherently unstable under aggradational conditions. Although externally driven increases in net deposition rate or flow frequency may alter the rate of change in channel stability, such allogenic forcings are additive to autogenic effects. Analysis suggests that channel-levee systems become progressively more sensitive to external forcing as they develop. Accordingly, some channels will remain stable despite allogenic forcing as they are too immature to avulse, whereas others will avulse independently of allogenic forcing because they are at their autogenic limit; the recent Amazon Fan avulsion record is consistent with this model.

Acknowledgments

This work is funded by the TRG consortium (Anadarko, BG-Group, BHP-Billiton, BP, Conoco Phillips, Marathon Oil, Maersk Oil, Nexen, Statoil, Tullow, and Woodside). We thank Ben Kneller, Gary Parker, Allesandro Cantelli, Ven Kolla, Jeff Peakall, David Hodgson, Mark Maslin, Eelcho Rohling, and two anonymous reviewers for their discussion and suggestions. Theoretical model derivation and long timescale solutions are available in the supporting information Text S1.

The Editor thanks an anonymous reviewer for his/her assistance in evaluating this paper.

References

- Audet, D. M. (1998), Mechanical properties of terrigenous muds from levee systems on the Amazon Fan, *Geol. Soc. London Spec. Publ.*, 129(1), 133–144.
- Buffington, E. C. (1952), Submarine “natural levees”, *J. Geol.*, 60(5), 473–479.
- Chiang, C. S., H. S. Yu, A. Noda, T. TuZino, and C. C. Su (2012), Avulsion of the Fangliao submarine canyon off southwestern Taiwan as revealed by morphological analysis and numerical simulation, *Geomorphology*, 177, 26–37.
- Covault, J. A. (2011), Submarine fans and canyon-channel systems: A review of processes, products and models, *Nat. Edu. Knowl.*, 3(10), 4.
- Clark, I. R., and J. A. Cartwright (2011), Key controls on submarine channel development in structurally active settings, *Mar. Pet. Geol.*, 28(7), 1333–1349.
- Damuth, J. E., R. D. Belderson, R. O. Flood, R. H. Kowsmann, and M. A. Gorini (1988), Anatomy and growth pattern of Amazon deep-sea fan as revealed by long-range side-scan sonar (GLORIA) and high-resolution seismic studies, *AAPG Bull.*, 72(8), 885–911.
- Deptuck, M. E., G. S. Steffens, M. Barton, and C. Pirmez (2003), Architecture and evolution of upper fan channel-belts on the Niger Delta slope and in the Arabian Sea, *Mar. Pet. Geol.*, 20(6), 649–676.
- Dorrell, R. M., A. J. Hogg, and D. Pritchard (2013), Polydisperse suspensions: Erosion, deposition, and flow capacity, *J. Geophys. Res. Earth Surf.*, 118, 1939–1955, doi: 10.1002/jgrf.20129.
- Dorrell, R. M., S. E. Darby, J. Peakall, E. J. Sumner, D. R. Parsons, and R. B. Wynn (2014), The critical role of stratification in submarine channels: Implications for channelization and long runout of flows, *J. Geophys. Res. Oceans*, 119, 2620–2641, doi: 10.1002/2014JC009807.
- Flood, R. D., et al. (1995), Proceedings of the ODP Program, Initial Reports 155, Ocean Drilling Program, College Station, Tex.
- Grant, K. M., E. J. Rohling, M. Bar-Matthews, A. Ayalon, M. Medina-Elizalde, C. Bronk Ramsey, C. Satow, and A. P. Roberts (2012), Rapid coupling between ice volume and polar temperature over the past 150,000 years, *Nature*, 491(7426), 744–747.
- Grant, K. M., et al. (2014), Sea-level variability over five glacial cycles, *Nat. Commun.*, 5(5076), 1–9.
- Jegou, I., B. Savoye, C. Pirmez, and L. Droz (2008), Channel-mouth lobe complex of the recent Amazon Fan: The missing piece, *Mar. Geol.*, 252(1), 62–77.
- Kane, I. A., and D. M. Hodgson (2011), Sedimentological criteria to differentiate submarine channel levee subenvironments: Exhumed examples from the Rosario Fm. (Upper Cretaceous) of Baja California, Mexico, and the Fort Brown Fm. (Permian), Karoo basin, S. Africa, *Mar. Pet. Geol.*, 28(3), 807–823.
- Kane, I. A., W. D. McCaffrey, J. Peakall, and B. C. Kneller (2010a), Submarine channel levee shape and sediment waves from physical experiments, *Sediment. Geol.*, 223(1), 75–85.
- Kane, I. A., W. D. McCaffrey, and J. Peakall (2010b), On the origin of paleocurrent complexity within deep marine channel levees, *J. Sediment. Res.*, 80, 54–66.
- Kneller, B. (2003), The influence of flow parameters on turbidite slope channel architecture, *Mar. Pet. Geol.*, 20(6), 901–910.
- Kolla, V. (2007), A review of sinuous channel avulsion patterns in some major deep-sea fans and factors controlling them, *Mar. Pet. Geol.*, 24(6), 450–469.
- Lopez, M. (2001), Architecture and depositional pattern of the Quaternary deep-sea fan of the Amazon, *Mar. Pet. Geol.*, 18(4), 479–486.
- Maslin, M. (2009), Review of the timing and causes of the Amazon Fan Mass Transport and avulsion deposits during the latest Pleistocene, in *External Controls on Deep-Water Depositional Systems*, vol. 92, edited by B. C. Kneller, O. J. Martinsen, and W. D. McCaffrey, SEPM Spec. Publ., Okla.
- Maslin, M., P. C. Knutz, and T. Ramsay (2006), Millennial-scale sea-level control on avulsion events on the Amazon Fan, *Quat. Sci. Rev.*, 25(23), 3338–3345.
- Miller, K. G., G. S. Mountain, J. D. Wright, and J. V. Browning (2011), A 180-million-year record of sea level and ice volume variations from continental margin and deep-sea isotopic records, *Oceanography*, 24, 40–53.
- Mohrig, D., and J. Buttles (2007), Deep turbidity currents in shallow channels, *Geology*, 35, 155–158.
- Peakall, J., W. D. McCaffrey, and B. C. Kneller (2000), A process model for the evolution, morphology, and architecture of sinuous submarine channels, *J. Sediment. Res.*, 70(3), 434–448.
- Pirmez, C., and R. D. Flood (1995), Morphology and structure of Amazon Channel, *Proc. Ocean Drill. Program Initial Reports*, 155, 23–45.
- Pirmez, C., and J. Imran (2003), Reconstruction of turbidity currents in Amazon Channel, *Mar. Pet. Geol.*, 20(6), 823–849.
- Pirmez, C., R. T. Beaubouef, S. J. Friedmann, and D. C. Mohrig (2000), Equilibrium profile and baselevel in submarine channels: Examples from Late Pleistocene systems and implications for the architecture of deepwater reservoirs, in *Deep-Water Reservoirs of the World: 20th Annual*, edited by P. Weimar et al., SEPM Foundation 20th Annual Bob F. Perkins Research Conference, Houston, Tex.
- Ramsey, C. B. (2009), Bayesian analysis of radiocarbon dates, *Radiocarbon*, 51(1), 337–360.
- Reimer, P. J., et al. (2013), IntCal13 and Marine13 radiocarbon age calibration curves 0–50,000 years cal BP, *Radiocarbon*, 55(4), 1869–1887.
- Saller, A., and I. N. W. Dharmasamadhi (2012), Controls on the development of valleys, canyons, and unconfined channel-levee complexes on the Pleistocene slope of East Kalimantan, Indonesia, *Mar. Pet. Geol.*, 29(1), 15–34.

- Sawyer, D. E., P. B. Flemings, and M. Nikolinakou (2014), Continuous deep-seated slope failure recycles sediments and limits levee height in submarine channels, *Geology*, *42*(1), 15–18.
- Silva, C. M. D. A. (2011), Controls on slope channel-levee evolution in the Amazon Fan, Doctoral dissertation, Univ. of Leeds, Leeds.
- Simpson, J. E. (1999), *Gravity Currents: In the Environment and the Laboratory*, Cambridge Univ. Press, Cambridge.
- Spinewine, B., T. Sun, N. Babonneau, and G. Parker (2011), Self-similar long profiles of aggrading submarine leveed channels: Analytical solution and its application to the Amazon channel, *J. Geophys. Res.*, *116*, F03004, doi: 10.1029/2010JF001937.
- Stanford, J. D., R. Hemingway, E. J. Rohling, P. G. Challenor, M. Medina-Elizalde, and A. J. Lester (2011), Sea-level probability for the last deglaciation: A statistical analysis of far-field records, *Global Planet. Change*, *79*(3), 193–203.
- Straub, K. M., and D. Mohrig (2008), Quantifying the morphology and growth of levees in aggrading submarine channels, *J. Geophys. Res.*, *113*, F03012, doi: 10.1029/2007JF000896.
- Straub, K. M., D. Mohrig, B. McElroy, J. Buttles, and C. Pirmez (2008), Interactions between turbidity currents and topography in aggrading sinuous submarine channels: A laboratory study, *Geol. Soc. Am. Bull.*, *120*(3-4), 368–385.
- Straub, K. M., D. Mohrig, J. Buttles, B. Pirmez, and C. McElroy (2011), Quantifying the influence of channel sinuosity on the depositional mechanics of channelized turbidity currents: A laboratory study, *Mar. Pet. Geol.*, *28*(3), 744–760.
- Wright, J. D., R. E. Sheridan, K. G. Miller, J. Uptegrove, B. S. Cramer, and J. V. Browning (2009), Late Pleistocene sea level on the New Jersey Margin: Implications to eustasy and deep-sea temperature, *Global Planet. Change*, *66*, 93–99.
- Wynn, R. B., B. T. Cronin, and J. Peakall (2007), Sinuous deep-water channels: Genesis, geometry and architecture, *Mar. Pet. Geol.*, *24*(6), 341–387.